Pham, H. Q., Fredlund, D. G. & Barbour, S. L. (2003). *Géotechnique* **53**, No. 2, 293–298

TECHNICAL NOTE

A practical hysteresis model for the soil–water characteristic curve for soils with negligible volume change

H. Q. PHAM,* D. G. FREDLUND* and S. L. BARBOUR*

KEYWORDS: constitutive relations; laboratory tests; partial saturation; suction

INTRODUCTION

The relationship between water content and suction in an unsaturated soil is called the *soil–water characteristic curve* (SWCC). The SWCC has been used to estimate the permeability and shear strength functions, which are subsequently used in the modelling of unsaturated soil behaviour (Fredlund & Rahardjo, 1993; Barbour, 1999). The SWCC of a soil is hysteretic, and the measurement of a complete set of hysteretic curves is extremely time-consuming and therefore quite costly. A simple model for predicting (or estimating) the hysteretic SWCC is needed. Most models presented in the literature require, directly or indirectly, at least two boundary hysteresis curves to predict the scanning curves (Philip, 1964; Hank *et al.*, 1969; Mualem, 1973, 1974, 1984; Dane & Wierenga, 1975; Scott *et al.*, 1983; Jaynes, 1985; Hogarth *et al.*, 1988; Nimmo, 1992; Kawai *et al.*, 2000). Consequently, it is important to establish a means of predicting the boundary wetting curve from the drying curve, and vice versa. A relatively simple empirical model for predicting the bounding hysteretic soil–water characteristic curves is proposed in this paper. The model requires limited data, and provides a reasonably accurate main (or 'boundary') curve.

THE FENG & FREDLUND (1999) MODEL

The Feng & Fredlund (1999) hysteresis model uses the soil–water characteristic curve-fitting equation to present both the boundary drying curve and the boundary wetting curve:

$$w(\psi) = \frac{w_u b + c\psi^d}{b + \psi^d} \tag{1}$$

In equation (1), the parameter c represents the water content at a relatively high soil suction. When w_u and c are constant, the parameter d represents the slope at the inflection point of the curve, and both parameters d and b control the *air-entry value*. Sample plots of equation (1) are presented in Fig. 1.

Equation (1) was developed based on measurements of the hysteresis associated with variable pore size ceramics (Feng & Fredlund, 1999) used in the construction of thermal conductivity suction sensors. The results showed that the entire boundary wetting curve could be predicted with only two points on the boundary wetting curve; however, the authors did not specify the positions of these points. Recommendations for the locations of the two points along the boundary wetting curve are presented in this paper.

Manuscript received 24 April 2002; revised manuscript accepted 11 November 2002.
Discussion on this paper closes 1 September 2003; for further details see p. ii.
* Department of Civil Engineering, University of Saskatchewan, Canada.

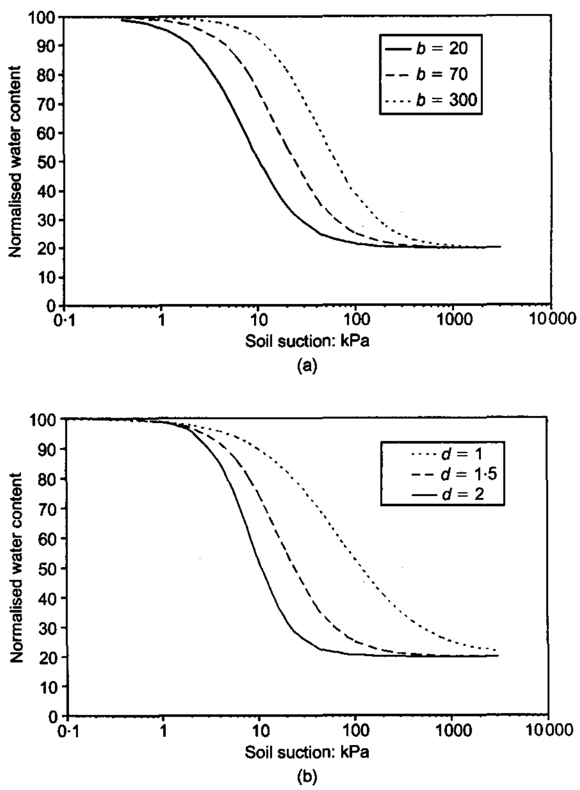

Fig. 1. Sample plots of equation (1) with $w_u = 100$, $c = 20$: (a) $d = 1{\cdot}5$ (b varies); (b) $b = 70$ (d varies)

SOIL DATA AND A STATISTICAL ANALYSIS

The data used to test hysteretic models for the SWCC were obtained from a laboratory study on two soils as well as from a database of 32 soils collected from the literature by Pham (2001). Information on the 32 soils is presented in Table 1, which includes six glass beads, a ceramic stone, 13 sands, six sandy loams, four silt loams and two clay loams. It is assumed that there is negligible volume change in soils upon the wetting and the drying processes.

Laboratory test programme

The two soils used in the laboratory test programme were Beaver Creek sand and processed silt from Saskatchewan, Canada. Samples of the two soils were compacted at water contents slightly lower than the optimum water content (that is, dry of optimum based on ASTM D-698). For each soil, three specimens were prepared, and the following hysteretic SWCCs were measured: the initial drying curve, the boundary wetting curve, and the boundary drying curve. All the

Table 1. List of collected soils

No.	Soil name	Reference
1	Adelaide dune sand	Talsma (1970)
2	Avondale clay loam	Watson *et al.* (1975)
3	Caribou silt loam	Topp (1971)
4	Ceramic (No. 1)	Feng (1999)
5	Coarse sand	Viaene *et al.* (1994)
6	Dune sand	Gillham *et al.* (1976)
7	Glass bead (4D)*	Nimmo & Miller (1986)
8	Glass bead (20D)*	Nimmo & Miller (1986)
9	Glass bead (35D)*	Nimmo & Miller (1986)
10	Glass bead (50D)*	Nimmo & Miller (1986)
11	Glass bead	Bomba & Miller (1967)
12	Glass bead ballotini (mixed)	Poulovassilis (1962)
13	Mixed sand fraction	Poulovassilis (1970b)
14	Mixed sand fraction	Poulovassilis & El-Ghamry (1978)
15	Molongo sand	Talsma (1970)
16	Norfolk sandy loam (15D)*	Hopmans & Dane (1986)
17	Norfolk sandy loam (32D)*	Hopmans & Dane (1986)
18	Packed sand	Vachaud & Thony (1971)
19	Plainfield sand loam (20D)*	Nimmo & Miller (1986)
20	Plainfield sand loam (35D)*	Nimmo & Miller (1986)
21	Plainfield sand loam (50D)*	Nimmo & Miller (1986)
22	Plano silt loam (4D)*	Nimmo & Miller (1986)
23	Plano silt loam (35D)*	Nimmo & Miller (1986)
24	Plano silt loam (50D)*	Nimmo & Miller (1986)
25	Porous body I (sand)	Poulovassilis (1970a)
26	Porous body II (sand)	Poulovassilis (1970a)
27	Rideau clay loam	Topp (1971)
28	Rubicon sandy loam	Topp (1969)
29	Sand	Poulovassilis & Childs (1971)
30	Sand (No. 17)	Perrens & Watson (1977)
31	Sand (R8)	Ayers & Watson (1977)
32	Wray dune sand	Mualem & Klute (1984)
33	Beaver Creek sand (compacted)	Laboratory test programme
34	Processed silt (compacted)	Laboratory test programme

* Some soils are tested at different temperatures: the notations 4D, 15D, 20D, 32D, 35D and 50D mean that the temperatures of the samples are 4, 15, 20, 32, 35 and 50°C respectively.

tests were performed using a pressure plate constructed at the University of Saskatchewan, Saskatoon, Canada. The testing procedures are the same as those used by Feng (1999). The test results show good agreement between the three identical specimens of each of the two soils. The average results of the three specimens were used to represent the data points from the laboratory test programme. It was found that equation (1) provided a satisfactorily fit to the actual data (Fig. 2).

Soil data collection

Thirty-two soil datasets of measured wetting and drying soil–water characteristic curves were collected from the research literature and were statistically analysed. This work is described in detail by Pham (2001). Only soils having at least two boundary hysteresis curves and a complete set of data over a wide range of soil suctions were collected. The hysteretic SWCCs were digitised using the Un-Scan-It computer software (Silk Scientific Corporation, 1998). This program allows data points to be obtained from a graph with user-defined coordinates. The dataset was stored in an Excel spreadsheet.

Statistical analysis

A statistical analysis was used to compare the slopes of the two boundary curves at the inflection point for the 34 soils. It was observed that the slope of the boundary drying curve was not very different from the slope of the boundary wetting curve using either an algebraic or a semi-logarithmic coordinate axis for soil suction. The ratios of the slope of the boundary wetting curve to the slope of the boundary drying curve using an algebraic and a semi-logarithmic coordinate axis for soil suction were in the range 0·48–1·74 and 0·96–3·40 respectively.

PROPOSED POSITIONS FOR THE TWO ADDITIONAL POINTS

Theory

In this section, the theory of the model for predicting a boundary (i.e. wetting or drying) curve using the opposite boundary (i.e. drying or wetting) curve is presented. Let us assume that one of the two boundary curves is measured in the laboratory. The residual water content and the water content at zero soil suction are known. These water contents are assumed to be essentially the same for both of the two boundary curves. Once one of the two boundary curves is measured, two parameters (i.e. w_u and $w_r \approx c$) in equation (1) can be defined from a best fit of the equation to the measured boundary curve.

Two additional curve-fitting parameters are required to predict the other boundary curve, b and d. In order to find these two curve-fitting parameters, two additional points on the opposite boundary curve are required. Generally, it is easier to measure the boundary drying curve than the boundary wetting curve. Therefore the application of the model to predict the boundary wetting curve from the boundary drying curve is presented.

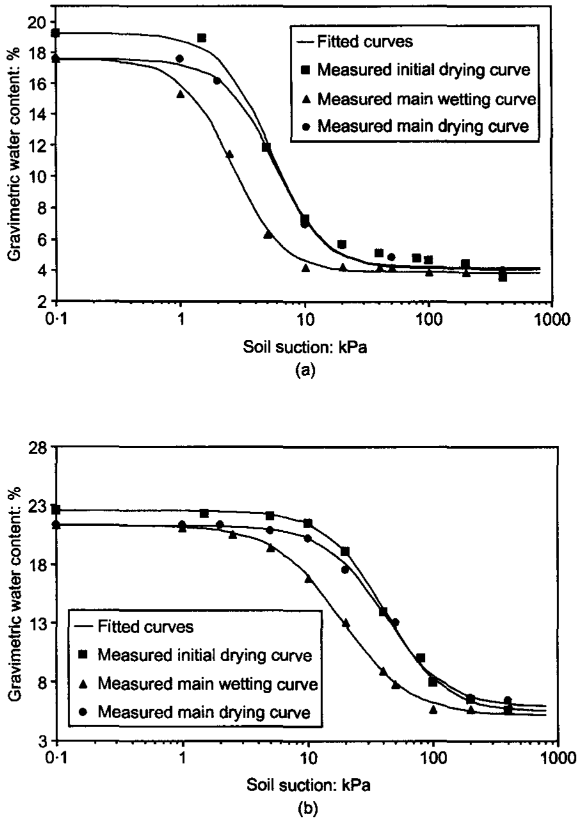

Fig. 2. Average hysteretic soil–water characteristic curves for: (a) Beaver Creek sand; (b) processed silt. The continuous lines are best fit using Feng & Fredlund (1999) equation

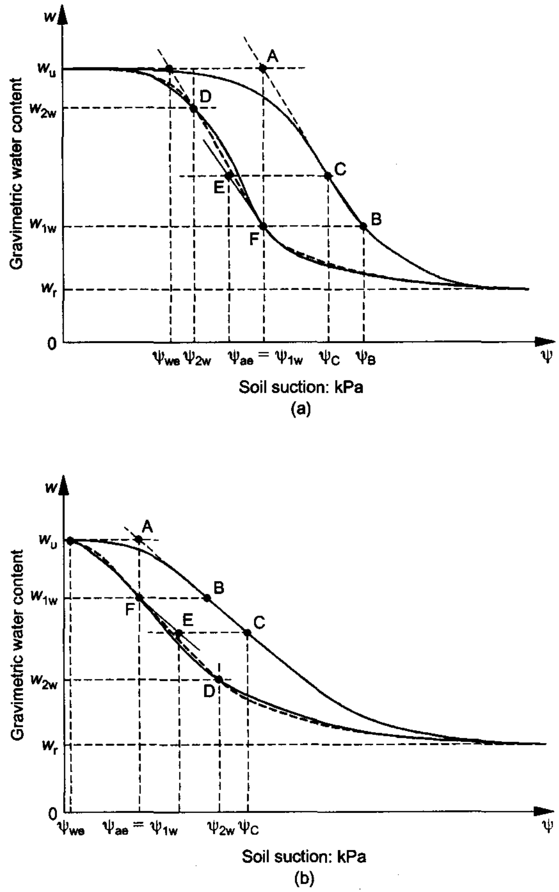

Fig. 3. Schematic illustrations of procedures of Feng & Fredlund (1999) model for predicting the boundary wetting curve: (a) case 1, water content at first point lower than that of inflection point; (b) case 2, water content at first point higher than that of inflection point. Continuous lines are measured curves; dashed lines are predicted curves

Once the boundary drying curve is measured, two additional points on the boundary wetting curve must be measured in order to predict the entire boundary wetting curve. Specific locations for these two additional points are proposed. The location of the first point on the boundary wetting curve can be selected as a soil suction close to the air-entry value of the boundary drying curve. It is suggested that the soil suction for the first point be approximated using the following equation, where b_d and d_d are curve-fitting parameters for the boundary drying curve:

$$\psi_{1w} \approx \left(\frac{b_d}{10}\right)^{1/d_d} \tag{2}$$

The soil suction of the second point on the boundary wetting curve can be chosen relative to the first point. The second point on the boundary wetting curve should be a point having a suction value that is symmetrical to the suction value of the first point about a vertical line passing through the inflection point of the boundary wetting curve (Fig. 3). Fig. 3 illustrates the method for estimating the location of the second point on the boundary wetting curve for the two typical shapes of the hysteretic SWCC (that is, the water content at the soil suction of the air-entry value on the boundary wetting curve is higher and lower than that of the inflection point of the boundary wetting curve). In order to locate the second point, the location of the inflection point of the boundary wetting curve needs to be determined. The statistical analysis of 34 soil datasets illustrated that the slope of the boundary wetting curve bears a similarity to the slope of the boundary drying curve. The inflection point of the boundary wetting curve can be estimated using the slope of the boundary drying curve and the first point on the boundary wetting curve.

Using the slope of the boundary drying curve for estimating the inflection point of the boundary wetting curve does not restrict the model to the prediction of a boundary wetting curve that is parallel to the boundary drying curve. Equations presenting soil suction values of the second point on the boundary wetting curve based on two different soil suction coordinates are presented in the next section.

Mathematical presentation

The soil suction and water content at the two additional points are defined as ψ_{1w}, w_{1w} and ψ_{2w}, w_{2w} respectively. The soil suctions at points B, C and E are ψ_B, ψ_C and ψ_E respectively (Fig. 3). Using the algebraic soil suction coordinate, the following equations can be established for calculating the soil suction (i.e. ψ_{2w}) of the second point on the boundary wetting curve:

$$|\psi_{2w} - \psi_E| = |\psi_{1w} - \psi_E| \tag{3}$$

$$|\psi_{1w} - \psi_E| = |\psi_B - \psi_C| \tag{4}$$

$$\psi_{\rm B} = \left[\frac{b_{\rm d}(w_{\rm u} - w_{\rm 1w})}{w_{\rm 1w} - c}\right]^{1/d_{\rm d}} \quad (5)$$

$$\psi_{\rm C} = b_{\rm d}^{1/d_{\rm d}} \quad (6)$$

The value of ψ_{2w} can be obtained by solving equations (3)–(6):

$$\psi_{\rm 2w} = \psi_{\rm 1w} - 2\left\{\left[\frac{b_{\rm d}(w_{\rm u} - w_{\rm 1w})}{w_{\rm 1w} - c}\right]^{1/d_{\rm d}} - b_{\rm d}^{1/d_{\rm d}}\right\} \quad (7)$$

Once these water contents at ψ_{1w} and ψ_{2w} are measured (i.e. w_{1w} and w_{2w}), the two unknown curve-fitting parameters b_w and d_w can be calculated for the boundary wetting curve:

$$d_{\rm w} = \frac{\log\left[\dfrac{(w_{\rm 1w} - c)(w_{\rm u} - w_{\rm 2w})}{(w_{\rm u} - w_{\rm 1w})(w_{\rm 2w} - c)}\right]}{\log(\psi_{\rm 2w}/\psi_{\rm 1w})} \quad (8)$$

$$b_{\rm w} = \frac{(w_{\rm 1w} - c)\psi_{\rm 1w}^{d_{\rm w}}}{w_{\rm u} - w_{\rm 1w}} \quad (9)$$

Similarly, on the semi-logarithmic soil suction coordinate, the following equations can be established for calculating the soil suction (i.e. ψ_{2w}) of the second point on the boundary wetting curve:

$$|\log(\psi_{\rm 2w}) - \log(\psi_{\rm E})| = |\log(\psi_{\rm 1w}) - \log(\psi_{\rm E})| \quad (10)$$

$$|\log(\psi_{\rm 1w}) - \log(\psi_{\rm E})| = |\log(\psi_{\rm B}) - \log(\psi_{\rm C})| \quad (11)$$

It is found that, using the algebraic soil suction coordinate, a unique equation (i.e. equation (7)) is obtained for the location of the second point on the boundary wetting curve. Using the semi-logarithmic soil suction coordinate, two equations are required to define the location of the second point on the boundary wetting curve (depending on the shape of the hysteretic SWCC). It is suggested that equation (7) be used for determining the location of the second point.

The prediction of the boundary drying curve from the boundary wetting curve and two points on the boundary drying curve can be implemented in a similar manner. The soil suction at the first point on the boundary drying curve can be chosen as a point having soil suction that is symmetrical to the *water-entry value* of the boundary wetting curve about the vertical line passing through the inflection point of the boundary wetting curve using the semi-logarithmic soil suction axis. The soil suction for the first point can be approximated using equation (12). Using the algebraic soil suction coordinate, the soil suction for the second point can be approximated using equation (13). The parameters b_w and d_w are curve-fitting parameters for the measured boundary wetting curve.

$$\psi_{\rm 1d} \approx (10 b_{\rm w})^{1/d_{\rm w}} \quad (12)$$

$$\psi_{\rm 2d} = \psi_{\rm 1d} - 2\left\{\left[\frac{b_{\rm w}(w_{\rm u} - w_{\rm 1d})}{w_{\rm 1d} - c}\right]^{1/d_{\rm w}} - b_{\rm w}^{1/d_{\rm w}}\right\} \quad (13)$$

Application

The proposed method of estimating the hysteretic SWCC will be illustrated using data for one of the soils tested in

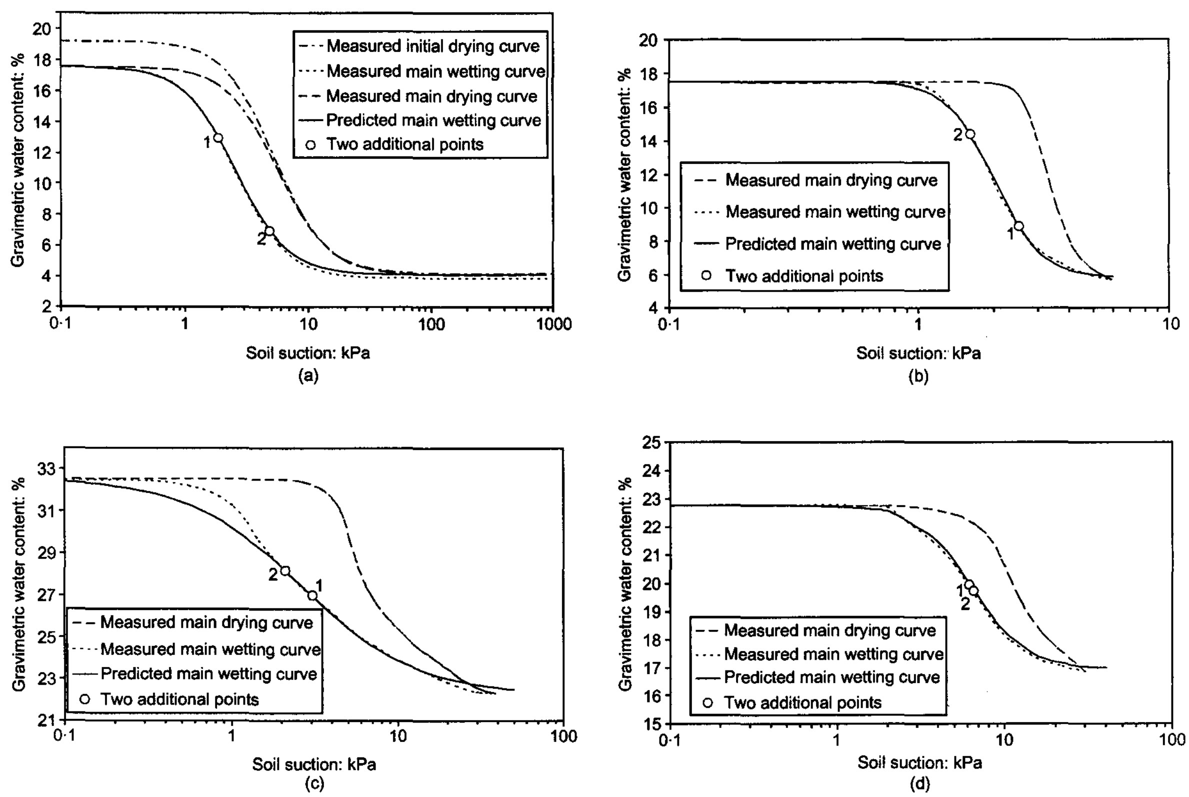

Fig. 4. Predicted and measured boundary wetting curves for: (a) Beaver Creek sand; (b) Dune sand (Gillham *et al.*, 1976); (c) Rideau clay loam (Topp, 1971); (d) Avondale clay loam (Watson *et al.*, 1975)

the laboratory programme (the Beaver Creek Sand) and for three of the hysteretic SWCCs collected from the literature: the Avondale clay loam (Watson *et al.*, 1975), the Dune sand (Gillham *et al.*, 1976) and the Rideau clay loam (Topp, 1971).

In order to predict the boundary wetting curve, the boundary drying curve is measured first. The water content at two additional points on the boundary wetting curve needs to be measured. The suction values at which these measurements should be made can be calculated using equations (2) and (7). Two unknown parameters, b_w and d_w, for the boundary wetting curve are calculated using equations (8) and (9). The fitted measured boundary curves and predicted curves for the four soils are plotted in Fig. 4.

DISCUSSION AND CONCLUSION

The results show that the boundary wetting curve predicted using the Feng & Fredlund (1999) model is quite close to the laboratory-measured results. At high soil suctions, the predicted boundary wetting curve is slightly overestimated in some cases. The error results from an insufficient number of measured data points on the boundary drying curve at and beyond the residual water content. The following should be undertaken to increase the accuracy of the model.

(*a*) Increase the number of measured data points at and beyond the residual water content.
(*b*) Choose the residual water content of the boundary wetting curve, c_w, to be equal to the water content of the point having the highest soil suction on the measured boundary drying curve.

The Feng & Fredlund (1999) model requires a relatively simple dataset for calibration. Unlike some previous hysteresis models, the positions of two additional points on the predicted boundary curve in the model are clearly defined based on experimental data (Pham, 2001). The model predicts the boundary curves quite well. The Feng & Fredlund (1999) curve-fitting equation is most applicable for low swelling soil.

NOTATION

b, c, d	curve-fitting parameters of an SWCC
b_d, d_d	curve-fitting parameters for the boundary drying curve
b_w, d_w	curve-fitting parameters for the boundary wetting curve
w_{1d}, w_{2d}	water content at the first and second additional points on the boundary drying curve
w_{1w}, w_{2w}	water content at the first and second additional points on the boundary wetting curve
w_u	water content at zero soil suction on the boundary curves
ψ_{1d}, ψ_{2d}	soil suction at the first and second additional points on the boundary drying curve
ψ_{1w}, ψ_{2w}	soil suction at the first and second additional points on the boundary wetting curve
ψ_B, ψ_C, ψ_E	soil suction at points B, C and E respectively

REFERENCES

Ayers, R. N. & Watson, K. K. (1977). Experimental and numerical studies of soil–water movement to a water table. *Proc. 6th Australasian Conf. Hydraulic and Fluid Mechanics, Adelaide*. Institution of Engineers, Australia, National Conference Publication 77, No. 12, 72–75.

Barbour, S. L. (1998). Nineteenth Canadian Geotechnical Colloquium: the soil–water characteristic curve, a historical perspective. *Can. Geotech. J.* **35**, No. 5, 873–894.

Bomba, S. I. & Miller, E. E. (1967). Secondary-scan hysteresis in glass-bead media. *Proc. Annual Mtng, Soil Science Society of America.*

Dane, J. H. & Wierenga, P. J. (1975). Effect of hysteresis on the prediction of infiltration, redistribution and drainage of water in layered soil. *J. Hydrol.* 1975, **25**, 229–242.

Feng, M. (1999). *The effects of capillary hysteresis on the measurement of matric suction using thermal conductivity sensors*. MSc thesis, University of Saskatchewan, Canada.

Feng, M. & Fredlund, D. G. (1999). Hysteretic influence associated with thermal conductivity sensor measurements. *Proceeding from Theory to the Practice of Unsaturated Soil Mechanics*, in association with 52nd Can. Geotech. Conf. & Unsaturated Soil Group, Regina, pp. 14:2:14–14:2:20.

Fredlund, D. G. & Rahardjo, H. (1993). *Soil mechanics for unsaturated soils*. New York: Wiley.

Gillham, R. W., Klute, A. & Heermann, D. F. (1976). Hydraulic properties of a porous medium: measurement and empirical representation. *Soil Sci. Soc. Am. J.* **40**, No. 2, 203–207.

Hank, R. J., Klute, A. & Bresler, E. (1969). A numerical method for estimating infiltration redistribution, drainage, and evaporation of water from soil. *Water Resour. Res.* **13**, 992–998.

Hogarth, W. L., Hopmans, J., Parlange, J. Y. & Haverkamp, R. (1988). Application of a simple soil-water hysteresis model. *J. Hydrol.* **98**, 21–29.

Hopmans, J. W. & Dane, J. H. (1986). Temperature dependence of soil water retention curves. *Soil Sci. Soc. Am. J.* **50**, 562–567.

Jaynes, D. B. (1985). Comparison of soil–water hysteresis models. *J. Hydrol.* **75**, 287–299.

Kawai, K., Karube, D. & Kato, S. (2000). The model of water retention curve considering effects of void ratio. *Proceedings Asian Conference on Unsaturated Soils*, pp. 329–334.

Mualem Y. (1973). Modified approach to capillary hysteresis based on a similarity hypothesis. *Water Resour. Res.* **9**, No. 5, 1324–1331.

Mualem, Y. (1974). A conceptual model of hysteresis. *Water Resour. Res.* **10**, No. 3, 514–520.

Mualem, Y. (1984). A modified dependent domain theory of hysteresis. *J. Soil Sci.* **137**, No. 5, 283–291.

Mualem, Y. & Klute, A. (1984). Predictor–corrector method for measurement of hydraulic conductivity. *Soil Sci. Soc. Am. J.* **48**, 993–1000.

Nimmo, J. R. (1992). Semi-empirical model of soil water hysteresis. *Soil Sci. Soc. Am. J.* **56**, 1723–1730.

Nimmo, J. R. & Miller, E. E. (1986). The temperature dependence of isothermal moisture vs potential characteristics of soils. *Soil Sci. Soc. Am. J.* **50**, 1105–1113.

Perrens, S. J. & Watson, K. K. (1977). Numerical analysis of two-dimensional infiltration and redistribution. *Water Resour. Res.* **13**, No. 4, 781–790.

Pham, Q. H. (2001). *An engineering model of hysteresis for soil-water characteristic curves*. MSc thesis, University of Saskatchewan, Canada.

Philip, J. R. (1964). Similarity hypothesis for capillary hysteresis in porous materials. *J. Geophys. Res.* **69**, No. 8, 1553–1562.

Poulovassilis, A. (1962). Hysteresis of pore water: an application of the concept of independent domains. *J. Soil Sci.* **92**, 405–412.

Poulovassilis, A. (1970a). Hysteresis of pore water in granular porous bodies. *J. Soil Sci.* **109**, No. 1, 5–12.

Poulovassilis, A. (1970b). The effect of entrapped air on the hysteresis curves of a porous body and on its hydraulic conductivity. *J. Soil Sci.* **109**, No. 3, 154–162.

Poulovassilis, A. & Childs, E. C. (1971). The hysteresis of pore water: the non-independence of domains. *J. Soil Sci.* **112**, No. 5, 301–312.

Poulovassilis, A. & El-Ghamry, W. M. (1978). The dependent domain theory applied to scanning curves of any order in hysteretic soil water relationships. *J. Soil Sci.* **126**, No. 1, 1–8.

Scott, P. S., Farquhar, G. J. & Kouwen, N. (1983). Hysteretic effects on net infiltration. In *Advances in infiltration* **11**, 163–170. St Joseph, MI: ASAE.

Talsma, T. (1970). Hysteresis in two sands and the independent domain model. *Water Resour. Res.* **6**, No. 3, 964–970.

Topp, G. C. (1969). Soil–water hysteresis measured in a sandy loam compared with the hysteretic domain model. *Soil Sci. Soc. Am. Proc.* **33**, 645–651.

Topp, G. C. (1971). Soil water hysteresis in silt loam and clay loam soils. *Water Resour. Res.* **7**, No. 4, 914–920.

Vachaud, G. & Thony, J.-L. (1971). Hysteresis during infiltration and redistribution in a soil column at different initial water content. *Water Resour. Res.* **7**, No. 1, 111–127.

Viaene, P., Vereecken, H., Diels, J. & Feyen, J. (1994). A statistical analysis of six hysteresis models for the moisture retention characteristic. *J. Soil Sci.* **157**, No. 6, 345–355.

Watson, K. K., Reginato, R. J. & Jackson, R. D. (1975). Soil water hysteresis in a field soil. *Soil Sci. Soc. Am. Proc.* **39**, No. 2, 242–246.